

Dynamical properties of the Lorentz gas

K. C. Sharma

*Department of Mathematics and Computer Science, Royal Military College, Kingston, Ontario, Canada K7K 5L0,
and Department of Physics, University of Guelph, Guelph, Ontario, Canada N1G 2W1*

S. Ranganathan

Department of Mathematics and Computer Science, Royal Military College, Kingston, Ontario, Canada K7K 5L0,

P. A. Egelstaff and A. K. Soper*

Department of Physics, University of Guelph, Guelph, Ontario, Canada N1G 2W1

(Received 14 January 1987)

A Lorentz gas interacting with a Lennard-Jones (LJ) potential and obeying classical equations of motion has been simulated by the molecular-dynamics method. A system of 255 Ar particles and one H₂ molecule at a reduced Ar density 0.413 and temperature 2.475 is simplified by allowing the "argon" to have infinite mass, and the hydrogen molecule interacts with Ar atoms via the LJ potential. The simulated incoherent dynamic structure factor $S_s(Q, \omega)$ for the hydrogen molecule, which is corrected for the rotational states, is found to be in reasonable agreement with the experimental data of Egelstaff *et al.* (unpublished). One-parameter phenomenological model calculations are also compared to these data.

I. INTRODUCTION

One fundamental problem of condensed-matter physics is the scattering of a light particle in a medium of heavy stationary scatterers, which is the "Lorentz-gas" (LG) model.¹ There has been interest in a classical particle moving in an environment of randomly distributed static scatterers, both at the theoretical² and experimental levels.^{3,4} The situation is simple when the distance between scatterers is large, and in the limiting case an exact solution is available^{1,5} based on the linearized Boltzmann equation. However, the problem becomes complicated as the scatterer density increases, so that the dynamic correlations start playing a role (including the memory effects) and the system attains the characteristics of a genuine many-particle fluid. The kinetic theory of this fluid, in the hard-sphere approximation, involves fundamental difficulties which increase considerably in the presence of "soft" interaction potentials.

Even though the dynamics of the host medium is absent, the LG system exhibits a number of interesting nontrivial features.⁶⁻¹⁰ A significant feature is a nonexponential decay of the velocity autocorrelation function (VAF) at long times, which indicates some nontrivial correlation effects present in the system.^{11,12} These long-time tails (with the VAF decaying according to some power law) are a general feature of transport in disordered diffusive systems, both classical and quantum mechanical. A variety of methods (Refs. 13 and 14) have been used to derive long-time tails. The molecular-dynamics (MD) simulation studies of Bruin¹² revealed that both the diffusivity and the VAF are nonanalytic functions of the density, yielding a percolation edge separating the phase with nonzero diffusivity from the one having no diffusion. This type of

phase transition has been detected rather convincingly in two- and three-dimensional LG models through MD simulation experiments.

Recently, Gotze *et al.*¹⁴ examined two- and three-dimensional LG systems of overlapping hard spheres and studied various characteristic features related to the density and velocity autocorrelation functions. These features emerge quite naturally from an analysis of either of the phases near the percolation edge,¹⁵ including the density variation of the long-time tail which proves to be consistent with the computer simulation.

In general, MD computer simulation^{16,17} has been carried out with the hard-sphere potential. No work exists which uses a realistic potential. The present work involves MD simulation studies of the incoherent dynamic structure factor $S_s(Q, \omega)$ of the LG system with the Lennard-Jones (LJ) potential.

From the experimental-neutron-scattering point of view the hydrogen molecule in argon is a good LG system because hydrogen is the lightest classical particle, it has an intrinsic neutron cross section much greater than that of argon, the neutron scattering from hydrogen is almost totally incoherent, and the inelastic component¹⁸ of the scattering is to a good approximation a convolution of the rotational, translational, and vibrational terms. For the problem in hand, one can ignore the vibrational component, and the wide separation of the rotational levels allows the translational term to be observed. In the experimental work¹⁹ used here, pure hydrogen gas at 298 psi pressure was studied first and found to behave as a perfect gas. Then argon was pumped into the vessel with the H₂ to raise the pressure to about 7498 psi. On this sample of the LG gas, neutron time-of-flight measurements were made. Since Ar is relatively invisible to neutrons, the dy-

namics of the hydrogen molecules were observed easily.

The hydrogen-argon system in the liquid phase has been studied^{20,21} by neutron scattering; for the dense gas phase, data are available from the neutron scattering experiments of McPherson and Egelstaff.⁴ Some indirect data on the dynamical behavior of the LG system over a wide range of densities are available through far-infrared absorption²² experiments. The new neutron scattering data¹⁹ on $S_s(Q, \omega)$ were measured at 113 angles from 5° – 100° for 30-meV neutrons, and cover several densities up to a density which is about half the density at the percolation edge. We work with the highest experimental density, and these data are expected to involve many physically important features of the high-density regime.

The plan of this paper is as follows. Section II describes the basic theory while Sec. III gives the details of the calculation. Molecular-dynamics results are compared with the experimental data in Sec. IV, and this comparison and model calculations are discussed in Sec. V.

II. THEORY

The incoherent scattering cross section of neutrons per hydrogen molecule may be written in the form^{18,20}

$$\begin{aligned} \frac{d^2\sigma}{d\Omega d\omega} &= \sum_{J,J'} \left(\frac{d^2\sigma}{d\Omega d\omega} \right)_{JJ'} \\ &= \sum_{J,J'} \frac{k}{k_0} a^2(Q, J, J') S_T(Q, \omega - \omega_{JJ'}) . \end{aligned} \quad (1)$$

Here the subscript J, J' represents the partial cross section for the rotational transition $J \rightarrow J'$. $\mathbf{Q} = \mathbf{k}_0 - \mathbf{k}$, is the momentum transfer in units of \hbar ; \mathbf{k}_0 and \mathbf{k} are the initial and final wave vectors, respectively. $\hbar\omega = \hbar^2(k_0^2 - k^2)/2m$ is the energy transferred to the system in the scattering process. $\hbar\omega_{JJ'} = B[J'(J'+1) - J(J+1)]$ represents the rotational energy gain with the quantum numbers J and J' . The Pauli principle requires that J be even when the total nuclear spin $I = I_1 + I_2$ of the hydrogen molecule is 0 (parahydrogen) and odd when I is 1 (orthohydrogen). B is the rotational constant. $a^2(Q, J, J')$ plays^{18,20} the role of an effective incoherent scattering length. In writing the above expression, the main approximation has been the

neglect of the dynamical coupling between the rotational motion and the translational motion of the molecule. For the gas at room temperature the ratio of ortho- to parahydrogen is about 3:1 and most of the molecules are in their ground state. Because of the spin dependence of the neutron-proton cross section, the ratio of the ortho to para scattering is about 6 for the incident energy of 30 meV used in these experiments. However, a large part of the para cross section is due to $J=0 \rightarrow 1$ inelastic scattering which has a low intensity at the scattering angles employed.

In a compact notation, the total incoherent dynamic structure factor may be expressed in the form of convolution

$$S_s(Q, \omega) = \int S_R(Q, \omega') S_T(Q, \omega - \omega') d\omega' , \quad (2)$$

where ω' corresponds to the rotational energy states of the hydrogen molecule, and $S_T(Q, \omega)$ and $S_R(Q, \omega)$ are the translational and rotational contributions. $S_R(Q, \omega)$ is calculated by the free-molecule expressions given by Young and Koppel¹⁸ or Sears²⁰ and the translational contribution $S_T(Q, \omega)$ will be dealt with by either the molecular-dynamics simulation method or a phenomenological model.^{23,24} The incoherent dynamic structure factor²⁵ $S_T(Q, \omega)$ is associated with the translational motion through the intermediate structure function $F_s(Q, t)$ by the relation

$$S_T(Q, \omega) = \frac{1}{2\pi} \int_{-\infty}^{\infty} F_s(Q, t) e^{i\omega t} dt , \quad (3)$$

with

$$F_s(Q, t) = \langle \rho_{-Q}^s(0) \rho_Q^s(t) \rangle , \quad (4)$$

where

$$\rho_Q^s = e^{i\mathbf{Q} \cdot \mathbf{R}} . \quad (5)$$

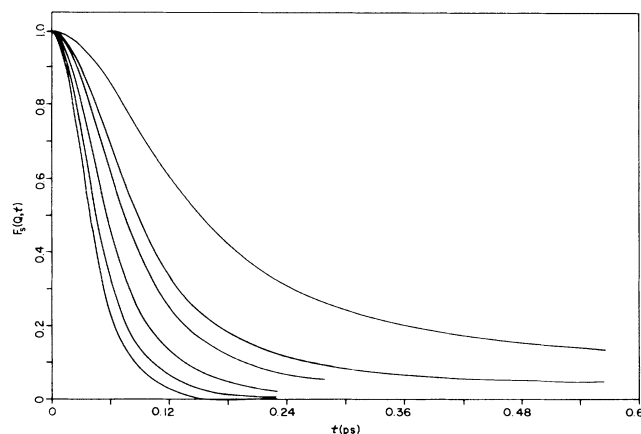


FIG. 1. Intermediate structure function $F_s(Q, t)$ vs t obtained from the MD calculation for $Q/Q_0 = 4, 6, 7, 9, 11$, and 13 . The slower decaying curves correspond to smaller values of Q .

TABLE I. Parameter used in the MD calculation of LJ gas.

	Parameters for the LJ potential	
	σ (Å)	ϵ/k_B (K)
Ar-Ar	3.405	120
H ₂ -Ar	3.168	64
Other parameters		
Temperature $T = 297$ K		
Total number of Ar particles 255; H ₂ molecules, 1		
Time $\tau_0 = (m\sigma_H^2/48\epsilon_H)^{1/2} = 8.87 \times 10^{-14}$ sec		
Reduced time increment $\Delta t^* = 0.032$ (in units of τ_0)		
Box length = $(N/n)^{1/3} = 29.0$ Å		
Reduced density $\rho^* = n\sigma_{Ar}^3 = 0.413$		

Here s indicates the quantity corresponding to the hydrogen molecule.

III. CALCULATIONS

A. Calculation of $S_T(Q, \omega)$ by molecular dynamics

The translational part of $S_s(Q, \omega)$ is calculated as follows. Argon atoms in the Lorentz-gas system are assumed to be of infinite mass and hence stationary. A hydrogen molecule is allowed to interact with Ar atoms through the LJ potential

$$\phi_i(r) = 4\epsilon \sum_j \left[\left(\frac{\sigma}{r_{ij}} \right)^{12} - \left(\frac{\sigma}{r_{ij}} \right)^6 \right], \quad (6)$$

where j corresponds to the Ar atom. The MD calculation was carried out for $N=256$ particles in a box with periodic boundary conditions, and the various parameters used are given Table I. An initial equilibrium configuration,²⁶ i.e., all three components of the position vector of N particles at a particular density and temperature, was obtained by the Monte Carlo method.²⁷ Then the hydrogen molecule was allowed to move at intervals of Δt^* in the static background of Ar atoms. The time is measured in terms of $\tau_0 = 8.87 \times 10^{-14}$ sec. The box length L was taken to be $\sim 29.0 \text{ \AA}$ with the reduced Ar density $n^* = 0.413$. Wave vectors for the MD run are integral multiples of $2\pi/L \sim 0.21 \text{ \AA}^{-1}$ which we denote by Q_0 . The calculation was performed for six values, $Q/Q_0 = 4, 6, 7, 9, 11,$ and 13 , but only four will be shown in the figures.

The initial velocity (three components) of the hydrogen molecule is obtained by choosing random speeds and random directions from the Maxwellian velocity distribution. Subsequent projections are obtained from the Verlet algorithm²⁸ and $\mathbf{r}(t)$ and $\mathbf{p}(t)$ are evaluated for 5000 time steps at time increments $\Delta t^* = 0.032$, from Newton's equations of motion. The intermediate structure function $F_s(Q, t)$ is then evaluated at equal time steps of Δt^* . In the calculation of $F_s(Q, t)$ every tenth time step is taken as the time origin and an average is taken over 500 time origins. Also, an average over 50 initial velocity configurations was taken and this gave an average temperature of 312 K. The calculated intermediate structure functions, $F_s(Q, t)$ for various Q 's, are plotted in Fig. 1.

The MD calculation has several limitations compared to the experiment. In the realistic (experimental) case the scatterers are of finite mass, compared to the infinite mass chosen for the calculations. The long-time tail represents ring and repeated-ring collisions, so one has to be very careful in choosing a proper cutoff to represent this effect. The $F_s(Q, t)$ data show the presence of some spurious fluctuations, though small in magnitude. A long-time tail appears particularly below 1.5 \AA^{-1} , and increases as Q decreases. The slow decay creates some inherent computational difficulty in getting $S_T(Q, \omega)$: For this reason we took a suitable cutoff point in time and extended the tail by an exponential decay. Thus it was possible to consider the long-time tail only approximately in the present calculation. Compared to an ideal LG gas which has a ran-

dom distribution of heavy scatterers, we have considered the equilibrium configuration of a real system at a particular density and temperature. This is proper as we are comparing with experimental results.

The relevant dynamic structure factor is then obtained after taking the Fourier transform,

$$S_T(Q, \omega) = \frac{1}{\pi} \int_0^\infty F_s(Q, t) \cos(\omega t) dt. \quad (7)$$

In the process, we tried to avoid the spurious fluctuations at long times, particularly at lower wave vectors, by choosing a suitable cutoff and extending the tail exponentially as $A \exp(-Bt)$. Then $F_s(Q, t)$ was multiplied by the experimental resolution function, $\exp(-0.82t^2)$ which is more important at lower values of the wave vector than at higher values of Q . For example, its effect at $Q = 0.867 \text{ \AA}^{-1}$ on the peak value of $S_s(Q, \omega)$ was found to be about 1%.

In a real system the H_2 molecule will exhibit some quantum rotational effects [see Eqs. (1) and (2)]. The translational contribution and the rotational contribution $S_R(Q, \omega)$ are convoluted to get the total incoherent contribution to the dynamic structure factor. Also there are some small effects which have been ignored as they are not expected to change the result by more than 1%. They include quantum effects on translation, the effect of H_2 -Ar coherent scattering, and many-body potential effects (i.e., beyond pair interactions). The first translational quantum correction would come from the terms of the type $e^{-\hbar^2 Q^2 / 2mk_B T}$ which will produce a correction at room temperature for large wave vectors, i.e., $Q > 3.0 \text{ \AA}^{-1}$, which are not considered in this paper.

B. Model calculation for $S(Q, \omega)$

We wish to calculate the translational contribution from a binary-collision model, such as the Nelkin-Ghatak²⁴ model. Calculations for two values of Q were compared to a simpler mathematical model of Egelstaff and Schofield²³ (ES) giving excellent agreement. Therefore the simple ES model was used for rest of the Q values. It assumes

$$F_s(Q, t) = \exp\left[-\frac{1}{2}\alpha(t)Q^2\right], \quad (8)$$

where $\alpha(t) \propto t^2$ in the short-time limit and $\alpha(t) = 2Dt$

TABLE II. Parameters used to calculate rotational contribution to $S_s(Q, \omega)$.

Temperature, 297 K
Molecular Mass 2
Bond length, 0.742 \AA
Rotational constant, 7.35 meV
Elastic energy, 30.97 meV
Neutron wavelength 1.625 \AA
Scattering length $a_0 = -0.374 \times 10^{-12}$ cm
Scattering length $a_1 = 5.82 \times 10^{-12}$ cm
Concentration of orthohydrogen, 75%
Maximum quantum number of rotational states, 11

within the diffusion approximation. Egelstaff and Schofield²³ proposed the expression

$$\alpha(t) = 2D[(t^2 + c^2)^{1/2} - c], \quad (9)$$

with $c = mD/k_B T$, which has the desired behavior at short and long times. It represents fairly well the molecular-dynamics results of Levesque and Verlet²⁹ on liquid Ar. Although it does not satisfy the fourth frequency moment of $S_s(Q, \omega)$, Lovesey³⁰ noted that the difference in $F_s(Q, t)$ is small. Thus the Egelstaff-Schofield²³ formula is a simple model involving one relaxation time. The situation can be different in a Lorentz gas at high density, where the long-time tail can be observed. After making this model calculation, the rotational contribution (see Table II) is incorporated as discussed in Sec. V.

IV. COMPARISON TO EXPERIMENT

A table of the experimental incoherent dynamic structure factor at 297 K, $S_s(Q, \omega)$, was available.¹⁹ The data, being measured at fixed scattering angles, were interpolated onto a constant- Q scale, and normalized by comparing pure-hydrogen-gas data to an appropriate calculation for

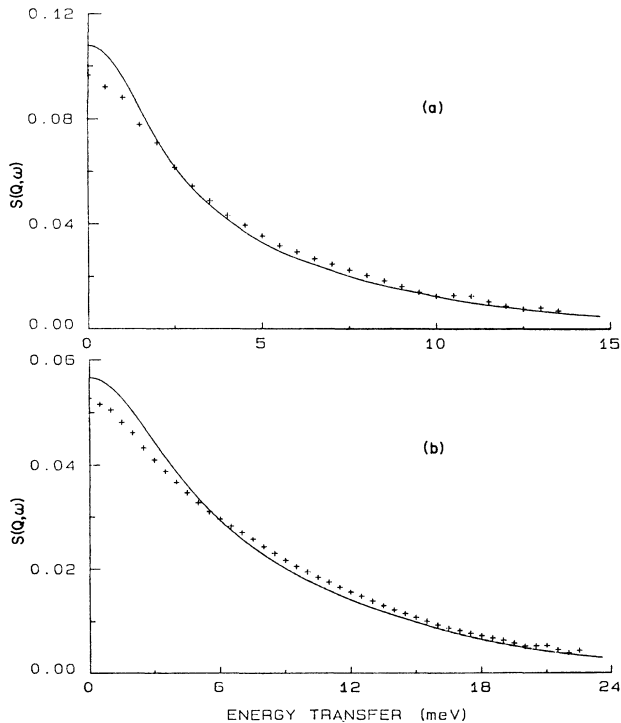


FIG. 2. Total incoherent dynamic structure factor $S_s(Q, \omega)$ vs ω of the Lorentz gas. Pluses represent the experimental data of Egelstaff *et al.* (Ref. 19). The solid line represents the present MD calculation. (a) $Q = 0.867 \text{ \AA}^{-1}$, (b) $Q = 1.300 \text{ \AA}^{-1}$.

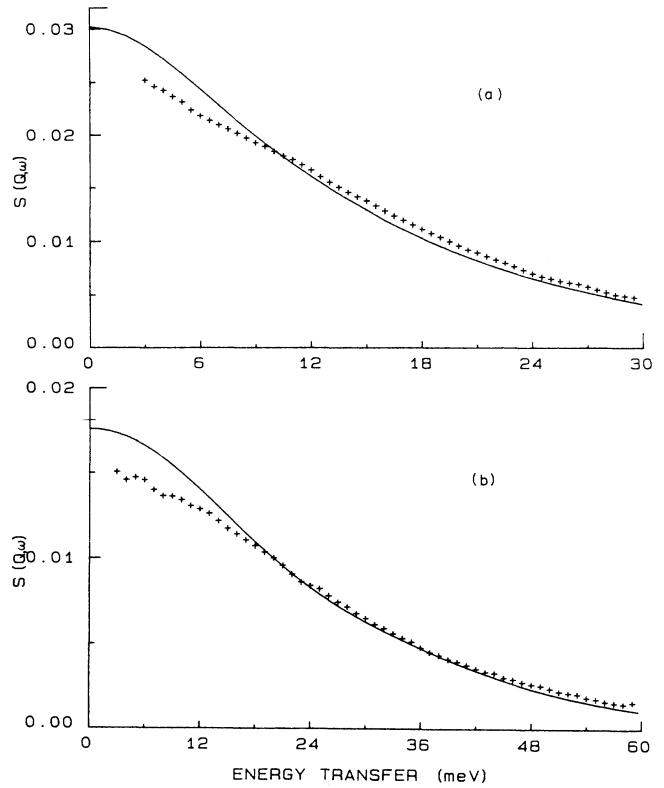


FIG. 3. Same as in Fig. 3. (a) $Q = 1.950 \text{ \AA}^{-1}$, (b) $Q = 2.818 \text{ \AA}^{-1}$. Data are omitted at low ω because of corrections for Bragg scattering.

the perfect gas, after correcting for resolution effects. A correction arising from the multiple scattering over the relevant range of energy transfers was evaluated and was found to be less than 2%.

The results obtained from the MD calculation of $S_T(Q, \omega)$, corrected for the rotational energy states of the hydrogen molecule, are presented in Figs. 2 and 3 and compared with the experimental data.¹⁹ Immediately, one observes that the MD calculation agrees fairly well with the data overall. However, near the zero-energy-transfer region, MD results show some disagreement. The region of disagreement for the lowest wave vector $Q = 0.867 \text{ \AA}^{-1}$ lies within $\omega < 1.5 \text{ meV}$. The MD peak value is larger by about 6% than the experimental value, and for these data the cutoff point in $F_s(Q, t)$ was chosen at $t = 0.34 \text{ ps}$ and the exponential decay was extended to 1.42 ps. If this cutoff is shifted to 0.57 ps, the MD peak further increases by about 7%, at the cost of smoothness in the $S_s(Q, \omega)$ plot. This probably indicates some contribution from the long-time tail of $F_s(Q, t)$, which is a manifestation of various ring collisions and other many-body effects.

The model of the Sec. III B was fitted to the experimental data by the least-squares method. The parameters obtained and quality of fit are shown in Figs. 4 and 5 and will be discussed in the Sec. V.

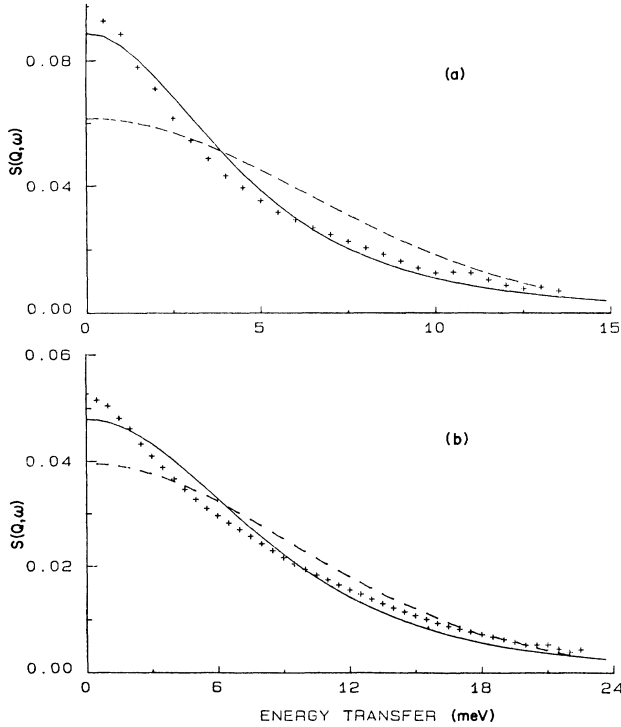


FIG. 4. Total incoherent dynamic structure factor $S_s(Q, \omega)$ vs ω of Lorentz gas. Pluses corresponded to the experimental result of Egelstaff *et al.* (Ref. 19) the solid line is the ES model, and the dashed line represents the perfect gas. (a) $Q=0.867 \text{ \AA}^{-1}$, $ck_B T/\hbar=3.34$; (b) $Q=1.300 \text{ \AA}^{-1}$, $ck_B T/\hbar=3.33$.

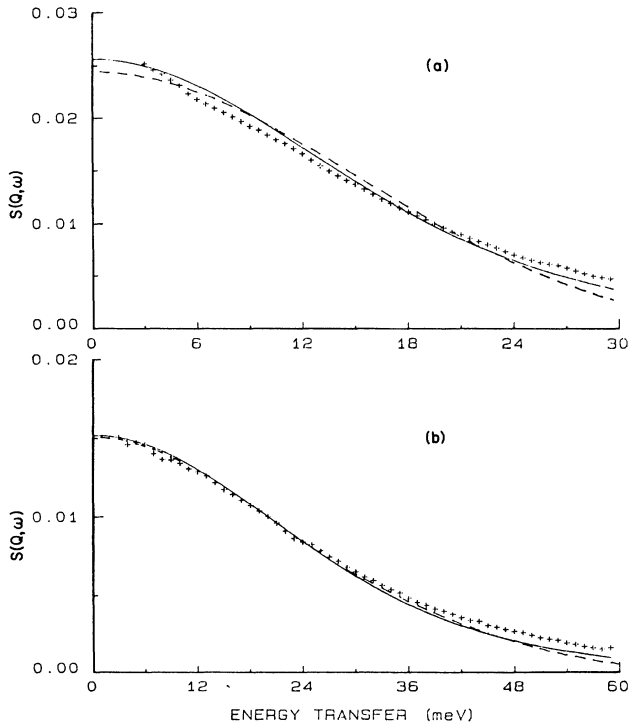


FIG. 5. Same as in Fig. 5. (a) $Q=1.950 \text{ \AA}^{-1}$, $ck_B T/\hbar=4.53$; (b) $Q=2.818 \text{ \AA}^{-1}$, $ck_B T/\hbar=5.60$. Data are omitted at low ω because of corrections for Bragg scattering.

V. DISCUSSION

In the molecular-dynamics simulation it was assumed that all the Ar atoms are of infinite mass so that they will not move, whatever energy is transferred from the hydrogen molecule on collision with the Ar atom. In a realistic system involving finite mass ($m=40$), the Ar atom moves and contributes to the width of $S_s(Q, \omega)$. Consequently, one can expect a sharper peak from MD simulation than the experimental one. This effect will be more evident at lower Q values.

We can obtain a quantitative assessment of the effect of the finite mass of argon, by letting the Ar atom move by normal dynamics and doing a MD calculation. However, to obtain a qualitative effect, we followed the kinetic arguments given by McPherson and Egelstaff.⁴ There are two related physical concepts which must be taken into account simultaneously. The mean free path, \bar{l}_1 , for a multicomponent gaseous mixture in the framework of the hard-sphere potential, may be expressed¹ as

$$\bar{l}_1 = \left[\pi \sum_s \rho_s \sigma_{1s}^2 g(\sigma_{1s}) (1 + m_1/m_s)^{1/2} \right]^{-1}, \quad (10)$$

where the subscript 1 represents the hydrogen molecule, m_s and ρ_s are the mass and the number density of the component s , σ_{1s} is the hard-sphere diameter at the 1- s contact, and $g(\sigma_{1s})$ is the pair distribution function at contact. In addition, we consider the "persistence of velocity."¹ The mean persistence ratio, defined as the mean of the ratio of the component of velocity after collision along the incident direction of velocity, to the velocity before the collision, is given¹ by

$$\bar{\omega}_{12} = \frac{1}{2} M_1 + \frac{1}{2} M_2 M_2^{-1/2} \ln[(m_2^{1/2} + 1)/m_1^{1/2}], \quad (11)$$

where $M_1 = m_1/(m_1 + m_2)$ and $M_2 = m_2/(m_1 + m_2)$. m_1 and m_2 are the masses of two different particles, i.e., the hydrogen molecule and the argon atom, in a binary gaseous system. The velocity vector is randomized after an average number of collisions \bar{n} , which we obtain from

$$\bar{n} = \frac{\sum_n n (\bar{\omega}_{12})^n}{\sum_n (\bar{\omega}_{12})^n}. \quad (12)$$

The effective mean free path for diffusion will be at most $\bar{l}_{\text{eff}} = \bar{l}_1 \bar{n}$ and the diffusion coefficient D can be expressed in terms of the above kinetic quantities, as

$$D = \frac{\bar{l}_{\text{eff}}^2}{6\tau} = \frac{\bar{l}_{\text{eff}} \bar{v}}{6} = \frac{\bar{l}_1 \bar{n} \bar{v}}{6}, \quad (13)$$

where τ is a suitable relaxation time, \bar{v} is the mean velocity and is $\sim \bar{l}_{\text{eff}}/\tau$. The product $\bar{l}_1 \bar{n}$ was calculated for $m_1/m_2 \rightarrow 0$ and for $m_1/m_2 = \frac{1}{20}$, and was found to be 1.58 and 1.59 \AA , respectively. As a check on these formulas we calculated the ratio of the relaxation time for a pure hydrogen system to that of a H_2 -Ar system. The result was about 2 [from Eq. (13)] compared with the experimental average value of 1.7 obtained from the work of McPherson and Egelstaff.⁴ Then, as a check on the value of \bar{l}_1 , we made a calculation with the parameter c of the ES model, which in units of $\hbar/k_B T$ is

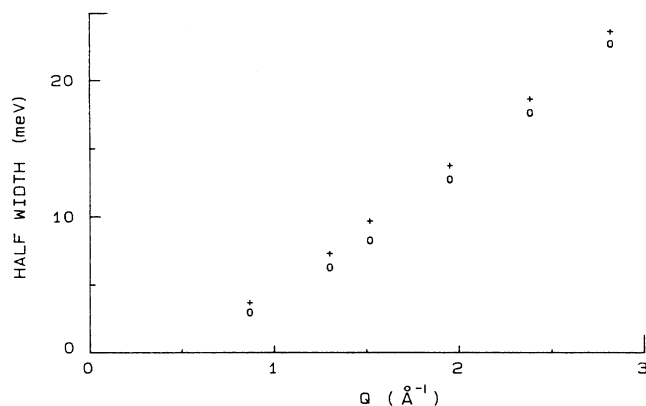


FIG. 6. Half-width (meV) vs Q (\AA^{-1}) of the Lorentz gas. Pluses represent the experimental data of Egelstaff *et al.* (Ref. 19). Open circles correspond to the present molecular dynamic calculation.

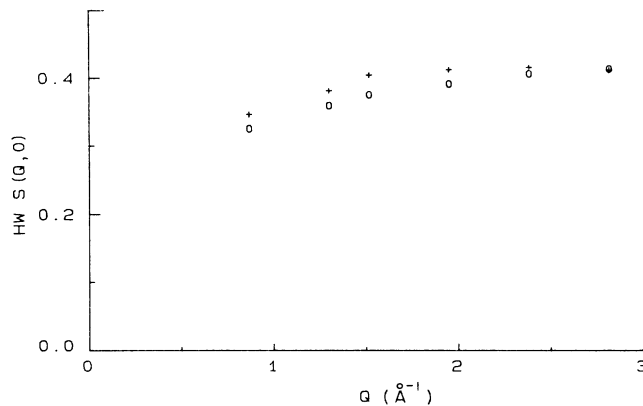


FIG. 7. Half-width (HW) times $S(Q,0)$ vs Q for the Lorentz gas. Various symbols are same as in Fig. 6.

$\bar{l}_1 \sqrt{Mk_B T/\hbar} \approx 3.3\bar{l}_1 \text{ \AA}$. We considered some typical average value of this parameter (see Figs. 4 and 5), i.e., ~ 4.7 , so that the mean free path comes out to be 1.4 \AA , which compares reasonably well with the value 1.5 \AA obtained from kinetic theory. This leads us to two conclusions: (a) the assumption of an infinite mass for argon is a good approximation, and (b) the finite mass of the scatterers, however, enhances the diffusion and hence the linewidth for large m_1/m_2 ratios.

The dynamic structure factors $S_s(Q, \omega)$ calculated from the Egelstaff-Schofield²³ model for four values of the wave vector Q , are compared with the experimental data in Figs. 4 and 5. The perfect-gas calculation is given also for reference. The model calculation lies between the perfect-gas result and the experimental data. The model has one parameter, namely diffusion, to cover the salient features of the system and also has only one relaxation time. The disagreement with the experiment (or with the MD calculation) suggests that a better model is needed.

Finally the half-width and half-width multiplied by $S(Q,0)$ versus Q are presented in Figs. 6 and 7, respectively. These results demonstrate clearly that the MD and experimental values are close to each other, in general, and also that they tend to follow the limiting behavior as $Q \rightarrow 0$ or $Q \rightarrow$ large values. At all Q 's, the MD cal-

ulation lies below the experimental data of Egelstaff *et al.*,¹⁹ in agreement with Figs. 2 and 3. Figure 7 shows that the data lie within the range obtained from the Ficks-law limit, $1/\pi$ (for $Q \rightarrow 0$) and the ideal-gas limit for ($Q \rightarrow \infty$). The latter is $\sqrt{\ln 2/\pi}$ times a rotational factor, to give a prediction of ~ 0.43 . This illustrates that the data we have been discussing cover the most sensitive range of Q .

The MD results are not sensitive to different equilibrium configurations of the host. Nevertheless, a random configuration of host atoms might have a significant effect, particularly near the zero-energy transfer region. We have not made any attempt to analyze the long-time tail of $F_s(Q, t)$ for small Q because a larger system is needed to discuss this important characteristic. It would be desirable to undertake further MD calculations which take account of these considerations and the effect of moving Ar atoms.

ACKNOWLEDGMENT

This research was supported, in part, by a grant from the Defense Research Board of Canada, Grant No. ARP-3610-774, and by a grant from the Natural Sciences and Engineering Researching Council of Canada.

*Present address: Rutherford Appleton Laboratory, Chilton, Oxon, England.

¹S. Chapman and T. G. Cowling, *The Mathematical Theory of Non-Uniform Gases*, 3rd ed. (Cambridge University Press, Cambridge, 1970).

²H. van Beijeen, *Rev. Mod. Phys.* **54**, 195 (1982), and references therein.

³A. S. M. Wahby and J. Los, *Physica* **128C**, 243 (1985).

⁴R. McPherson and P. A. Egelstaff, *Can. J. Phys.* **58**, 289 (1980).

⁵E. A. Mason, *J. Chem. Phys.* **27**, 782 (1957).

⁶J. M. J. van Leeuwen and A. Weyland, *Physica* **36**, 457 (1967).

⁷A. Weyland, J. M. J. van Leeuwen, *Physica* **38**, 35 (1968).

⁸M. H. Ernst and A. Weyland, *Phys. Lett.* **34A**, 39 (1971).

⁹A. Weyland, *J. Math. Phys.* **15**, 1942 (1974).

¹⁰J. C. Lewis and J. A. Tjon, *Phys. Lett.* **66A**, 349 (1978).

¹¹J. Machta, *J. Stat. Phys.* **42**, 941 (1986).

¹²C. Bruin, *Phys. Rev. Lett.* **29**, 1670 (1972); *Physica* **72**, 261 (1974).

¹³A. K. Harrison and R. Zwanzig, *J. Stat. Phys.* **42**, 935 (1986).

¹⁴W. Gotze, E. Leutheusser, and S. Yip, *Phys. Rev.* **23**, 2634 (1981); **24**, 1008 (1981); **25**, 533 (1982).

¹⁵E. H. Hauge, in *What Can One Learn From Lorentz Models*, Vol. 31 of *Lecture Notes in Physics*, edited by G. Kirczenow and J. Marro (Springer, Berlin, 1974), p. 337.

- ¹⁶B. J. Alder and W. E. Alley, *J. Stat. Phys.* **19**, 341 (1978).
- ¹⁷B. J. Alder and W. E. Alley, *Physica* **121A**, 523 (1983).
- ¹⁸J. A. Young and J. U. Koppel, *Phys. Rev.* **135**, A603 (1964).
- ¹⁹P. A. Egelstaff, O. J. Eder, W. Glaser, J. Polo, B. Renker, and A. K. Soper (unpublished).
- ²⁰V. Sears, *Proc. Phys. Soc.* **86**, 953 (1965); **86**, 965 (1965).
- ²¹O. J. Eder, S. H. Chen, and P. A. Egelstaff, *Proc. Phys. Soc.* **89**, 833 (1966).
- ²²J. C. Lewis, in *Phenomena Induced by Intermolecular Interactions*, edited by G. Birnbaum (Plenum, New York, 1985).
- ²³P. A. Egelstaff and P. Schofield, *Nucl. Sci. Eng.* **12**, 260 (1962).
- ²⁴M. Nelkin and A. Ghatak, *Phys. Rev.* **135**, A4 (1964).
- ²⁵P. A. Egelstaff, *An Introduction to the Liquid State* (Academic, New York, 1967).
- ²⁶G. M. Torrie (private communication).
- ²⁷J. P. Valleau and S. G. Whittington, in *Statistical Mechanics I*, edited by B. J. Berne (Plenum, New York, 1977).
- ²⁸L. Verlet, *Phys. Rev.* **159**, 98 (1967).
- ²⁹D. Levesque and L. Verlet, *Phys. Rev. A* **2**, 2514 (1970).
- ³⁰S. W. Lovesey, *J. Phys. C* **6**, 1856 (1973); in *Dynamics of Solids and Liquids by Neutron Scattering*, edited by S. W. Lovesey and T. Springer (Springer-Verlag, Berlin, 1977).